

Using Transformer Parasitics for Resonant Converters – A Review of the Calculation of the Stray Capacitance of Transformers

J. Biela, J. W. Kolar
Power Electronic Systems Laboratory (PES), ETH Zurich
Zurich, Switzerland
E-Mail: biela@lem.ee.ethz.ch / Homepage: www.pes.ee.ethz.ch

Abstract – Parasitic capacitances of conventional transformers can be used as resonant elements in resonant DC-DC converters in order to reduce the overall system size. For predicting the values of the parasitic capacitors without building the transformer different approaches for calculating these capacitances are compared. A systematic summary of the known approaches is given and missing links between the different theories and missing equations are added. Furthermore, a new simple procedure for modelling parasitic capacitances which is based on the known approaches is proposed. The resulting equations are verified by measurements on four different high voltage transformers.

Keywords: Transformer model, inductor model, parasitic capacitance, resonant converter, high voltage transformer

I. INTRODUCTION

Applying resonant DC-DC converters can help to reduce the switching losses and / or to raise the switching frequency of the power switches. On this account the overall system size in many industrial applications, e.g., telecom power supplies [1], high voltage generators [2] or inductive heating [3] could be reduced.

Especially, the series-parallel resonant converter, **Fig. 1**, is a promising converter structure since it combines the advantages of the series resonant and the parallel resonant concept. On the one hand the resonant current decreases with the decrease of the load and the converter can be regulated at no load and on the other hand good part-load efficiency can be achieved [4, 5]. Furthermore, the converter is naturally short circuit proof.

In order to reduce the overall system size the series inductance of the resonant circuit could be integrated into the transformer by increasing the transformer leakage inductance by a magnetic shunt as described in [6, 7]. Also the series and the parallel capacitor can be integrated in the transformer by using planar cores together with layers of high permittivity material [7 - 9]. The application of integrated planar cores, however, is limited to power levels up to some kilowatts and is not appropriate for high voltage applications. There, conventional transformers with wire winding structures are usually used. These transformers also have parasitic capacitances which can be used as integrated parallel capacitor of the resonant circuit.

Different aspects of the calculation of the parasitic capacitance are described in [10-51] but a complete structured overview and a comparison of the different calculation methods is missing. This will be presented and completed by deriving missing equations in this paper in order to find the most appropriate algorithm for calculating the “parasitic” parallel capacitance of the transformer and to find the winding structure which is most suitable for realising high capacitance

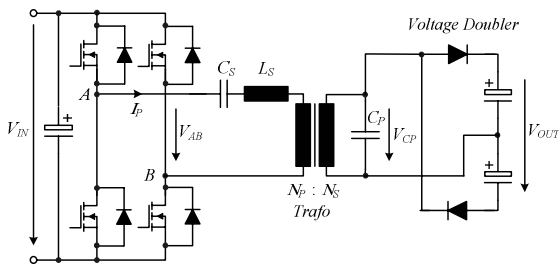


Figure 1. Series-parallel resonant DC-DC converter

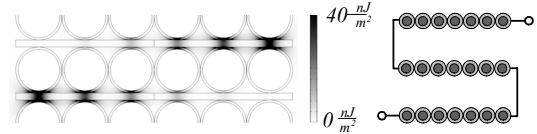


Figure 2. Energy distribution within a multilayer standard winding

values and which causes the lowest dielectric losses. Furthermore, the links and dependencies of the different approaches will be revealed.

In high voltage applications the number of turns of the secondary winding, which mainly causes the parasitic capacitance C_p , is high in order to limit the voltage per turn and to achieve a high step-up ratio. This fact and the insulation requirements usually result in multilayer and multi-section windings. For this reason the presented algorithms focus on the calculation of the parasitic capacitance of multilayer windings which are divided into one or more sections. As shown in **Fig. 2** the stored electric energy for a standard multilayer winding mainly concentrates between two successive layers. In comparison to that the energy between two turns of the same layer is very small. Thus, the turn-to-turn capacitances of turns in the same winding layer are neglected in this paper.

The equivalent capacitance of single layer coils, whose value mainly depends on the turn-to-turn capacitance, is not covered in this paper but information could be found in [47 - 51] for example.

All the parasitic capacitance models of windings/transformers are based on the static layer-to-layer capacitance, which could be measured at dc conditions between different layers. There are five different models for the static capacitance presented in literature - two simple approximations: parallel-plate capacitor [10] / cylindrical capacitor and three analytical methods [11, 12]. These models and the calculation methods are described in **section II** for windings consisting of solid or litz wire. With the equations for the static layer-to-layer capacitance the equivalent capacitor of standard and flyback windings (cf. Fig. 7 & 9) and with it a general equivalent model of multilayer windings could be calculated as presented in **section III**. This equivalent model also includes incomplete layers. The presented model is verified by FEA simulation results and is approximately valid just below the first resonant frequency of the winding [18] since it sums up distributed capacitances to a lumped capacitor.

In **section IV** a more general model of two winding layers, which could also be used to describe two layers of different windings or interleaved windings, is discussed. The results of the different approaches are verified by measurements of the parasitic capacitance of four different high voltage transformers in **section V**. Finally, a conclusion and topics of future research are given in **section VI**.

II. STATIC CAPACITANCE MODEL

All calculations of the equivalent winding capacitance are based on the static layer-to-layer capacitance. With this capacitance the electrical energy is calculated which is stored between two successive winding layers and which will be used in section 3 for calculating the equivalent capacitance. The layer-to-layer capacitance is calculated by assuming that the layers of the winding are equipotential surfaces i.e. that all turns of one layer are short-circuited and edge effects are neglected. Thus, two successive layers of the winding could be

approximated by a cylindrical capacitor (**Fig. 4b**) or a parallel-plate capacitor (**Fig. 4a**).

A. Parallel-Plate Capacitor Model

For calculating the static capacitance there are five different approaches. The first one replaces the round wires by flat rectangles as shown in **Fig. 3**. In a second step the flat rectangles can be replaced by an equipotential surface if the electrical connection between the layers is disconnected and dc conditions are assumed. This results in a parallel-plate capacitor as shown in Fig 5a [10].

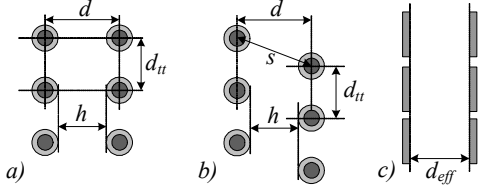


Figure 3 (a) Orthogonal winding (b) Orthocyclic winding (c) Definition of effective distance between plates

The distance d_{eff} is the effective distance between the plates (cf. Fig.3c). It is determined by calculating the capacitance of the real arrangement of the wires (Fig. 3a or 3b) i.e. the capacitance of the two wire grids and the value of the parallel-plate capacitor (Fig. 4a). By equating these two capacitance values the effective distance d_{eff} could be calculated (cf. (1)) as a function of the geometry of the wire grid. The variable d' is given in (2) for orthogonal windings (cf. section II.C) and in (3) for orthocyclic windings (cf. section II.D). For the orthocyclic winding there are two different values for d' depending on the distance of the two layers.

$$d_{eff} = d' - 2.3 \cdot (r_0 + \delta) + 0.26 \cdot d_{tt} \quad (1)$$

$$\text{Orthogonal (3a): } d' = d = 2 \cdot r_0 + h \quad (2)$$

$$\text{Orthocyclic (3b): } d' = \begin{cases} d = 2 \cdot r_0 + h & h > 0 \\ r_0 + \frac{h}{2} + \frac{\sqrt{(2r_0 + h)^2 + \frac{d_{tt}^2}{4}}}{2} & h \leq 0 \end{cases} \quad (3)$$

The derivation of the relationship for the effective distance is described in [13] and it will not be repeated in this paper for the sake of brevity.

The value of the parallel-plate capacitor could be calculated as

$$C_{0,pla} = \epsilon_0 \cdot \epsilon_{r,m} \cdot \frac{l_{w,m} \cdot L_L}{d_{eff}} = \epsilon_0 \cdot \epsilon_{r,m} \cdot \frac{l_{w,m} \cdot z \cdot 2 \cdot r_0}{d_{eff}} \quad (4)$$

By (5) the effective permittivity $\epsilon_{r,m}$ and the average turn length of the two layers $l_{w,m}$ which are used in (4) can be calculated. The effective permittivity is determined by equating the voltage across the series connected dielectrics and the voltage across the equivalent dielectrics or by equating the stored energies [52].

$$\epsilon_{r,m} = \frac{\epsilon_D \cdot \epsilon_F \cdot (\delta + h)}{\epsilon_F \cdot \delta + \epsilon_D \cdot h}; \quad h = R_{2,cyl} - R_{1,cyl}; \quad l_{w,m} = \pi(R_{1,cyl} + R_{2,cyl}) \quad (5)$$

Remark: The author of [22] uses the parallel-plate capacitor model for approximating the relative permittivity by measurement data for wires

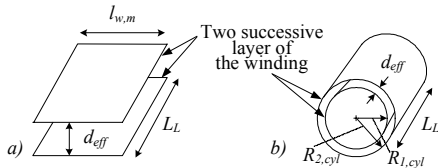


Figure 4. (a) Parallel-plate capacitor model (b) Cylindrical capacitor model

in the range $r_0 = 0.05..0.35\text{mm}$. The result is that ϵ_R varies from 1.3 for thicker wires to 2.2 for thinner ones for orthogonal windings (cf. Fig.3a). For orthocyclic windings the permittivity is assumed to approximately double. Furthermore, the author assumes that in a standard winding approximately half of the turns are orthogonal and the other half is orthocyclic. With the foregoing assumptions and by assuming further that $h = 0$ the resulting static interlayer capacitance is equal to

$$C_{0,app} \approx 180e^{-12} \cdot l_{w,m} \cdot \frac{z(z+1)(2z+1)}{6z^2} \approx 60 \cdot l_{w,m} z \quad [pF] \quad (z \gg 1) \quad (6)$$

This equation could be used as a rule-of-thumb for a first guess on the parasitic capacitances of windings.

B. Cylindrical Capacitor Model

Many windings have a cylindrical shape. Therefore, the second approach replaces the parallel-plate capacitor by a cylindrical capacitor as shown in **Fig. 4b**. Thereby, the round wires of a layer also have been replaced by equipotential surface (cf. section II.A / Fig. 3). For the cylindrical capacitor the capacitance is calculated by

$$C_{0,cyl} = \frac{\epsilon_0 \epsilon_{r,m} 2\pi L_L}{\ln\left(\frac{R_{1,cyl} + d_{eff}}{R_{1,cyl}}\right)} = \frac{\epsilon_0 \epsilon_{r,m} 2\pi z r_0}{\ln\left(\frac{R_{1,cyl} + d_{eff}}{R_{1,cyl}}\right)} \quad (7)$$

The radius of the inner cylinder is given as mean value of the two cylindrical layers minus half of the effective distance d_{eff} .

$$R_{1,cyl} = \frac{R_{L1} + R_{L2} - d_{eff}}{2} \quad (8)$$

For standard values for $R_{1,cyl}$ and $R_{2,cyl}$ of high power transformers the difference between the parallel-plate and the cylindrical capacitor model is quite small so that the simpler parallel-plate capacitor model could be used in most cases.

C. Analytic Capacitance Model for Orthogonal Windings

The remaining three approaches approximate the electric flux lines by straight lines. An example of an approximated electric flux line for an orthogonal winding, whose layers are separated by a foil of thickness h , is shown in the basic cell of **Fig. 5**. In orthogonal windings the turns of successive layers are orthogonally on top of each other, whereas in orthocyclic windings the turns of the successive layer are in the gaps between two turns of the preceding layer.

The electric flux line leaves the wire, which is an equipotential surface, approximately orthogonally. Because of the small thickness δ of the insulation the flux line approximately runs as a straight line to the border of the insulation [11]. Then the approximated flux line deviates towards the successive layer and runs as a straight line to the second layer. It crosses the symmetry line (dashed line in Fig. 5) of the two layers orthogonally. The path of the flux line continues symmetrically from the symmetry line to the second wire. This approach is used for all angles φ from 0 to 180° i.e. that within one basic cell all approximated electric flux lines from one turn to the underlying one are contained.

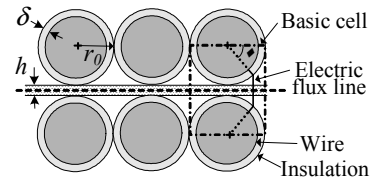


Figure 5. Analytic field calculation for orthogonal winding

In **Fig. 6** the resulting flux lines of a finite element analysis are shown. The FEA-flux lines correspond quite well with the approximated flux lines especially in the regions where the stored electric energy and

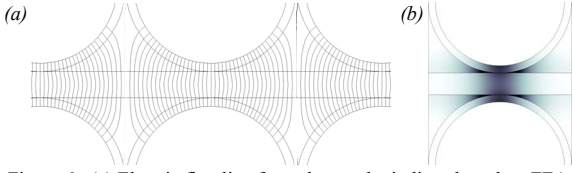


Figure 6. (a) Electric flux line for orthogonal windings based on FEA
(b) Distribution of electric field strength

therefore the parasitic capacitance is high (φ is around 90° - cf. Fig. 2 - energy).

With the considered path of the flux lines, a given permittivity of the insulation and the foil and the given voltage between one wire and the underlying wire (layer-to-layer voltage) the electric field strength in the different sections of the approximated flux line could be calculated. Then, the electric field strength could be used for calculating the electric energy which is stored between the two wires lying on top of each other. This energy is equated to the electric energy which is stored in the equivalent capacitor what leads to the equivalent capacitance of the basic cell. Multiplying this capacitance by the number of turns per layer z results in the static capacitance of the two layers. The detailed calculation is described in [11].

The result of the above described calculation is the static layer-to-layer capacitance for orthogonal windings

$$C_{\theta,ortho} = \frac{\epsilon_0 \cdot z \cdot l_{w,m}}{1 - \frac{\delta}{\epsilon_D \cdot r_0}} \cdot \left[V + \frac{1}{\delta \cdot \epsilon_D} \cdot \left(\frac{2 \cdot \delta}{r_0} \right)^2 \cdot \frac{Z}{1 - \frac{\delta}{\epsilon_D \cdot r_0}} \right] \quad (9)$$

with

$$V = \frac{\beta}{\sqrt{\beta^2 - 1}} \cdot \arctan \left(\sqrt{\frac{\beta+1}{\beta-1}} \right) - \frac{\pi}{4}$$

$$Z = \frac{\beta \cdot (\beta^2 - 2)}{(\beta^2 - 1)^{3/2}} \cdot \arctan \left(\sqrt{\frac{\beta+1}{\beta-1}} \right) - \frac{\beta}{2 \cdot (\beta^2 - 1)} - \frac{\pi}{4} \quad (10)$$

$$\alpha = 1 - \frac{\delta}{\epsilon_D \cdot r_0} ; \quad \beta = \frac{1}{\alpha} \cdot \left(1 + \frac{h}{2 \cdot \epsilon_F \cdot r_0} \right)$$

D. Analytic Capacitance Model for Orthocyclic Windings

A similar analytic approach [11] could be used for an orthocyclic winding which is shown in Fig. 7. There, the basic cell consists of a triangle (A-B-D) and the path of the approximated electric flux line, which is very similar to the one described in the foregoing section, is given. Again, the analytic electric flux lines correspond very well with the flux lines resulting from finite element analysis (Fig. 8).

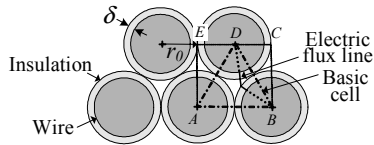


Figure 7. Analytic field calculation for orthocyclic winding

For calculating the static layer-to-layer capacitance the analytic flux line is used to calculate the energy which is stored in the basic cell as done in section II.C. In order to calculate the complete electric energy which is stored between one turn of the upper layer and the two underlying turns of the lower layer one also has to consider the energy stored in the two small triangles (A-D-E and B-C-D in Fig. 7). This is done by multiplying the energy stored in the basic cell by two since the two small triangles are half of the two adjacent basic cells.

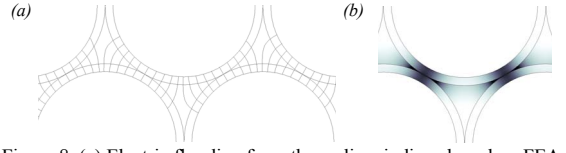


Figure 8 (a) Electric flux line for orthocyclic windings based on FEA
(b) Distribution of electric field strength

Again, the complete layer-to-layer capacitance is calculated by a comparison of stored energies (cf. section II.C). The resulting capacitance is

$$C_{\theta,cyclic} = 4 \cdot \epsilon_0 \cdot z \cdot l_{w,m} \cdot \left[M_L + \frac{4 \cdot \delta \cdot r_0 - 2 \cdot \delta^2}{\epsilon_D \cdot (2 \cdot r_0)^2} \cdot M_D \right] \quad (11)$$

together with

$$M_L = \int_0^{\pi/6} \frac{\cos^2 \psi - \cos \psi \cdot \sqrt{\cos^2 \psi - \frac{3}{4} - \frac{1}{2}}}{2 \left[\cos \psi - \left(1 - \frac{\delta}{2 \epsilon_D r_0} \right) \left(\sqrt{\cos^2 \psi - \frac{3}{4} + \frac{1}{2}} \right) \right]^2} d\psi$$

$$M_D = \int_0^{\pi/6} \frac{\sin^2 \psi + \cos \psi \cdot \sqrt{\cos^2 \psi - \frac{3}{4}}}{2 \left[\cos \psi - \left(1 - \frac{\delta}{2 \epsilon_D r_0} \right) \left(\sqrt{\cos^2 \psi - \frac{3}{4} + \frac{1}{2}} \right) \right]^2} d\psi \quad (12)$$

Remark: In order to achieve a better agreement between the calculations and measurements the authors of [21] introduced an empiric equation for the relative permittivity in (11).

$$\epsilon_D = 2.5 + \frac{0.7}{\sqrt{2 \cdot r_i / \text{mm}}} \quad (13)$$

With this function ϵ_D varies from 2.95 for $r_i = 1.25\text{mm}$ to 6 for $r_i = 0.02\text{mm}$.

E. 2nd Analytic Capacitance Model for Orthocyclic Windings

In [12] a second calculation model for the turn-to-turn capacitance of orthocyclic windings is presented. The approach is very similar to the one in the foregoing section except for the exact path of the electrical flux line and the shape of the basic cell as shown in Fig. 9 where the basic cell is a rhombus (e.g. A-B-C-D).

$$C_{\theta,cyclic II} = z \epsilon_0 l_{w,m} \frac{4 \epsilon_r \tan^{-1} \left[\frac{(\sqrt{3} - 1) \left(2 \epsilon_r + \ln \frac{r_0}{r_i} \right)}{(\sqrt{3} + 1) \sqrt{\ln \frac{r_0}{r_i} \left(2 \epsilon_r + \ln \frac{r_0}{r_i} \right)}} \right]}{\sqrt{2 \epsilon_r \ln \frac{r_0}{r_i} + \left(\ln \frac{r_0}{r_i} \right)^2}} \quad (14)$$

In order to calculate the complete energy stored between one turn of the lower layer and two "half" turns of the upper layer one has to consider two rhombuses (A-B-C-D and B-F-E-C). The area covered by these two rhombuses is a little bit smaller than the one covered by the two triangles of Fig. 7 and the path of the flux line in the region

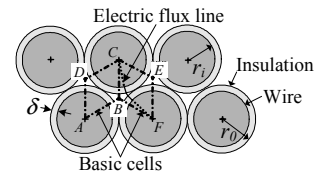


Figure 9. 2nd Analytic field calculation for orthocyclic winding

between the insulations of the wire is a bit different. Furthermore, for calculating (11) and (12) the author of [11] made some numerical approximations. This causes slight differences in the result for the static layer capacitance compared to (11).

F. Comparison of Static Layer Models

In **Table I** the results of the different models for the static interlayer capacitance and the result of a FEA-Simulation are compared. For the orthogonal windings all models yield good results. The results for the orthocyclic winding, however, show that the parallel-plate and the cylindrical plate model cause large errors since the models do not consider the reduced distance between the layers for orthocyclic windings.

A. Orthogonal Winding

FEA: 51.8pF/m	Value	Error
Parallel-Plate (4)	54.2pF/m	5.1 %
Cylindrical (7)	54.5pF/m	4.6 %
Orthogonal (9)	49.2pF/m	-4.9 %

B. Orthocyclic Winding

FEA 136.5pF/m	Value	Error
Parallel-Plate (4)	54.2pF/m	-60.2 %
Cylindrical (7)	54.5pF/m	-60 %
Orthocyclic (11)	140pF	2.8%
Orthocyclic II (14)	158pF	16.8%
Orthocyclic – Empiric (11+13)	146pF/m	7.8 %

TABLE I- Comparison between layer capacitance models with $l_{w,m} = 1m$; $\delta = 100\mu m$; $r_0 = 0.5mm$; $z = 1$; $h = 0.15mm$; $\epsilon_D = 3$; $\epsilon_F = 3$

Remark: A too exact modelling of the path of the electric flux lines and the static interlayer capacitance is useless since the tolerances of the geometric winding parameters are usually large and the positioning of the wire is not deterministic.

G. Using Litz Wire Instead of Solid Wire

For calculating the static interlayer capacitance C_0 the outer diameter r_0 of the wire and the nominal diameter d_i are needed. In order to apply the calculations also for inductors and transformers using litz wire these parameters have to be derived from the specifications of the applied litz wires as described in [21]. In **Fig. 10** the geometry of a litz wire and the belonging solid wire are depicted.

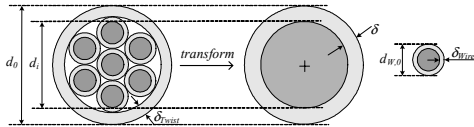


Figure 10. Transformation of litz-wire to solid wire

The nominal diameter d_i could be calculated by subtracting the thickness of the twists' outer insulation and the thickness of the insulation of a single strand from the outer diameter of the complete litz wire (15).

$$r_i = r_0 - \delta = r_0 - \delta_{Twist} - \delta_{Wire} \quad (15)$$

The outer diameter of the litz wire could be taken from the data sheet of the wire or calculated by (16) presented in [21].

$$r_0 = \sqrt{\frac{4N_S}{\pi} \cdot \frac{d_{W,0}}{2}} \quad (16)$$

Another possibility is to use (17) for determining the outer diameter. This equation is presented in [16] and is based on the interpolation of values given in data sheets of different litz wires.

$$r_0 = \frac{135 \cdot 10^{-6}}{2} \cdot \left(\frac{N_S}{3}\right)^{0.45} \cdot \left(\frac{d_{W,0} - 2\delta_{Wire}}{40 \cdot 10^{-6}}\right)^{0.85} - \delta_{Twist} \quad (17)$$

In general, the accuracy of the analytic calculation procedure for determining the equivalent capacitance of inductors or transformers using litz wire is limited since the winding tension and the shape of the bobbin strongly affect the parasitic capacitance of the winding. Further information on this topic could be found in [21].

III. CONNECTION OF LAYERS OF THE SAME WINDING

The static layer-to-layer capacitance does not comprise the voltage distribution between the layers which is dependent on the winding method (standard or flyback - cf. Fig. 7 & 9). According to the applied winding structure the effective layer-to-layer capacitance changes because the static capacitance is not charged uniformly but the charge distribution depends on the voltage distribution.

A. Standard Winding Method (Two Layers)

For the standard winding method (**Fig. 11**) one side ($x = 0$) of the two layers is shortened and the voltage between the two layers at the other side ($x = L_L$) is double the layer Voltage V_{Wdg}/N_{Layer} (it is assumed that all layers have the same number of turns z per layer). This fact leads to relatively high electric field strengths and dielectric losses at the unconnected side ($x = L_L$) of the layer.

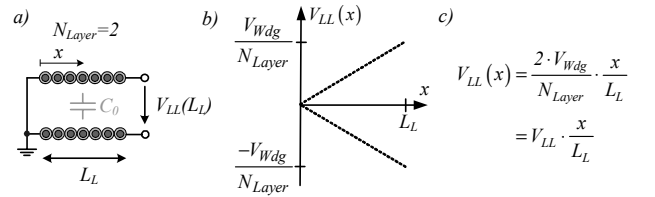


Figure 11. Layer-to-layer voltage for standard winding method

If it is assumed that all turns of the two layers comprise the same magnetic flux the voltage distribution along the layer (cf. Fig. 11c) is approximately linear (exact: staircase-shaped).

In this case the leakage flux, which flows through single turns of the layers, is neglected because it is very small for usual winding designs. With the voltage distribution $V_{LL}(x)$ the stored electric energy could be calculated as (where $V_{LL} = V_{Wdg}$)

$$W_{E,LL} = \frac{C_0}{2 \cdot L_L} \cdot \int_0^{L_L} V_{LL}^2(x) dx = \frac{2 \cdot C_0}{3} \left(\frac{V_{Wdg}}{N_{Layer}} \right)^2 = \frac{C_{Layer} \cdot V_{Wdg}^2}{2} \quad (18)$$

Equating this energy to the energy stored in the equivalent layer capacitor C_{Layer} (r.h.s. of (18)) results in the equivalent layer capacitor for the standard winding method $C_{Layer} = C_0/3$.

B. Flyback Winding Method (Two Layers)

With the flyback winding method all layers are wound in the same direction and the voltage between the two layers is constantly equal to the layer Voltage V_{Wdg}/N_{Layer} (**Fig. 12**). Therefore, the electric field strength and the dielectric stress is uniformly distributed and the dielectric losses are lower compared to the standard winding method.

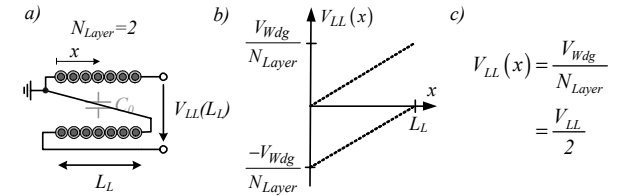


Figure 12. Layer-to-layer voltage for a flyback winding

A disadvantage of the flyback winding method is that at the end of one layer the wire of the winding has to cross all turns of this and the proximate layer. This leads to a larger overall winding length and to local high electric field strengths and dielectric losses (locally comparable to the standard winding method). The problem with the local high electric field strength could be avoided with special

arrangements of the "flyback connection" of the layers but this increases the complexity of the manufacturing significantly.

For calculating the voltage distribution (Fig. 12c) along the layer it is assumed again that all turns of the two layers are linked with the same flux (cf. section III.A).

Equating the stored electric energy (19 - where $V_{LL} = V_{Wdg}$) to the energy which is stored in the equivalent layer capacitor

$$W_{E,LL} = \frac{C_0}{2 \cdot L_L} \int_0^{L_L} V_{LL}^2(x) dx = \frac{C_0}{2} \left(\frac{V_{Wdg}}{N_{Layer}} \right)^2 = \frac{C_{Layer} \cdot V_{Wdg}^2}{2} \quad (19)$$

results in equivalent capacitor $C_{Layer} = C_0/4$.

C. General Approach for Arbitrary Winding Methods (Two Layers)

In sections III.A and III.B the voltage distribution between the two layers and therewith the equivalent layer capacitance is calculated separately for the standard and the flyback winding method. In the following a more general approach for arbitrary winding connections, which is used by many authors [e.g. 10], is presented.

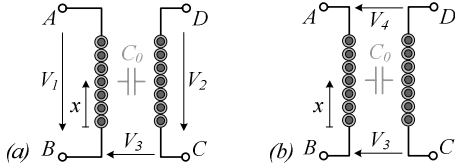


Figure 13. Layer-to-layer voltage for a flyback winding

The voltage between the two layers could be expressed in terms of V_1 , V_2 and, V_3 or V_3 and V_4 independently from the winding method (Fig. 13 and (20)).

$$V_{LL}(x) = V_3 + (V_2 - V_1) \cdot \frac{x}{L_L} = V_3 + (V_4 - V_3) \cdot \frac{x}{L_L} \quad (20)$$

With the layer voltage the stored energy is calculated and equated to the energy in the equivalent capacitance (cf. section III.A) what results in (21) for the equivalent capacitance where V_{LL} is the sum of the voltages across the two layers.

$$C_{Layer} = \frac{C_0}{3} \cdot \frac{(V_3^2 + V_3 \cdot V_4 + V_4^2)}{V_{LL}^2} = \frac{C_0}{3} \left((V_2 - V_1)^2 + 3V_3(V_2 - V_1) + 3V_3^2 \right) \quad (21)$$

Connecting the layers either with the standard or the flyback winding method the general approach provides the same results as calculated in sections III.A and III.B.

D. Multilayer Windings

In the preceding sections the calculation of the equivalent capacitance for two layers for different winding methods is described. With these equations the equivalent capacitance for multilayer windings with standard or flyback winding method (cf. Fig. 14) could be calculated as explained in the following.

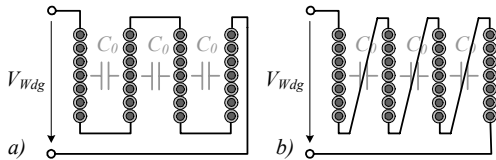


Figure 14. Multilayer standard (a) and flyback (b) winding method ($N_{Layer} = 4$)

Again, the equivalent capacitor for the complete winding is calculated by equating the energy stored in this capacitor to the energy which is stored in all the layer capacitors

$$W_{E,Wdg} = \frac{C_{Wdg} \cdot V_{Wdg}^2}{2} = \frac{1}{2} \cdot \sum_{v=1}^{N_{Layer}-1} C_{Layer,v} \cdot \left(\frac{2 \cdot V_{Wdg}}{N_{Layer}} \right)^2 \quad (22)$$

$$\Rightarrow C_{Wdg} = \sum_{v=1}^{N_{Layer}-1} C_{Layer,v} \cdot \left(\frac{2}{N_{Layer}} \right)^2 \quad (22)$$

If all layer capacitors $C_{Layer,v}$ are equal the equation for the equivalent winding capacitor simplifies to the well known equation

$$C_{Wdg} = 4 \cdot \frac{N_{Layer} - 1}{N_{Layer}^2} \cdot C_{Layer} \quad (23)$$

In (22) the calculation of the equivalent winding capacitor C_{Wdg} is done by equating the stored energies. A different approach uses the impedance transformation rule of auto-transformers. There, the equivalent layer capacitor of two layers $C_{i,i+1}$ is transformed into a capacitor at the input of the winding $C'_{i,i+1}$ by multiplying the equivalent layer capacitor $C_{i,i+1}$ by the square of the turns ratio of the two layers to the complete winding resulting in

$$C'_{i,i+1} = \frac{(N_{L,i} + N_{L,i+1})^2}{\left(\sum_{k=1}^{N_{Layer}} N_{L,k} \right)^2} \cdot C_{i,i+1} \Rightarrow C_{Wdg} = \sum_{i=1}^{N_{Layer}-1} C'_{i,i+1} \quad (24)$$

The transformed equivalent capacitors are connected in parallel and can be summed up to the equivalent winding capacitor C_{Wdg} , which is in parallel to the winding.

E. Incomplete Layers

So far only complete layers with z turns in each layer have been considered. In the following a winding with $N_{Layer}-1$ Layers with z turns and the last layer with $k < z$ turns is considered as shown in Fig. 15 / [21].

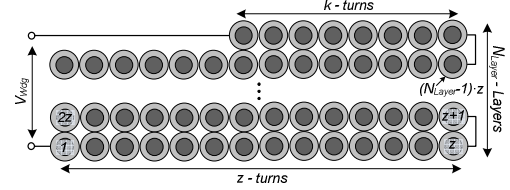


Figure 15. Winding with incomplete layer

The interlayer capacitance for the complete layers could be calculated as described in section III and the interlayer capacitance built by one complete and the incomplete layer scales linearly with the number of turns as shown in

$$C_{Layer,N} = C_{Layer} \cdot \frac{k}{z} \quad \text{with} \quad N = N_{Layer} - 1 \quad (25)$$

The equivalent winding capacitor C_{Wdg} is calculated by transforming all interlayer capacitors to the connection of the winding by the impedance transformation rule of transformers

$$C_{Wdg} = \frac{C_{Layer,N} \cdot 2k^2 + \sum_{v=0}^{N_{Layer}-2} C_{Layer,v} \cdot 2z^2}{\left((N_{Layer} - 1)z + k \right)^2} \quad (26)$$

If it is assumed that all interlayer capacitances are the same the equation simplifies to

$$C_{Wdg} = \frac{4 \cdot C_{Layer} \cdot (N_{Layer} - 1) \cdot (z^2 + k^2)}{\left((N_{Layer} - 1) \cdot z + k \right)^2} \quad (27)$$

IV. GENERAL MODEL OF TWO LAYERS

In section III an equivalent circuit for two or more layers of the same winding is calculated whereas in this section a model for two arbitrary successive layers is presented. This model could be used for calculating the equivalent capacitor of two layers from different

windings e.g. primary and secondary winding or interleaved winding structures.

A. Generalised Capacitance Model of Two Layers

As the authors of [14] have shown the electrostatic behaviour of a transformer (what is equivalent to two layers of different windings) could be modelled by a three input multipole (primary and secondary voltage and the voltage between the windings). In the linear working area and as long as propagation times can be ignored, the electrostatic energy / behaviour of this multipole could be modelled by six independent capacitors as shown in Fig. 16.

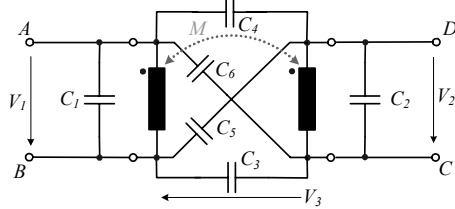


Figure 16. Equivalent circuit of two arbitrary layers/windings

The values of the six capacitors in Fig. 16 are again calculated by the energy approach. First, the energy which is stored in the capacitance between the two layers - cf. Fig. 13a - is calculated using the equation of the layer-to-layer voltage (20). The energy is expressed in terms of the three voltages V_1 , V_2 and, V_3 in

$$W_{E,LL} = \frac{C_0}{6} \left((V_2 - V_1)^2 + 3V_3(V_2 - V_1) + 3V_3^2 \right). \quad (28)$$

Secondly, also the energy stored in the six capacitors of Fig. 16 is calculated in dependence of V_1 , V_2 and, V_3 in

$$W_{E,6C} = \frac{1}{2} \left(C_1 \cdot V_1^2 + C_2 \cdot V_2^2 + C_3 \cdot V_3^2 + C_4 \cdot (V_2 + V_3 - V_1)^2 + C_5 \cdot (V_2 + V_3)^2 + C_6 \cdot (V_3 - V_1)^2 \right). \quad (29)$$

By equating these two energies and comparing the coefficients of the variables V_1 , V_2 , V_3 , $V_1 \cdot V_2$, $V_1 \cdot V_3$ and $V_2 \cdot V_3$ the six capacitors could be expressed in terms of the static winding capacitance C_0 . The result is given in (30). The values of these six capacitors can also be determined by three independent measurements as described in [14, 15] (where $C_1 = C_2$, $C_3 = C_4$ and $C_5 = C_6$ is assumed).

$$\begin{aligned} W_{E,LL} &= W_{E,6C} \\ \Rightarrow C_1 &= C_2 = -\frac{C_0}{6}; \quad C_3 = C_4 = \frac{C_0}{3}; \quad C_5 = C_6 = \frac{C_0}{6} \end{aligned} \quad (30)$$

B. Complete Capacitance Model for Transformers or Coils

With the equivalent circuit for arbitrary layers of different windings it is now possible to model the complete winding structure of transformers. Each pair of successive layers is modelled with an equivalent circuit consisting of six capacitors (Fig. 16) [17]. The result is a quite complex model of the parasitic winding capacitance if the number of layers is larger than two. However, it is always possible to reduce the number of equivalent capacitors to six as it is shown below.

In the following the transformer assembly in Fig. 17 is taken as an example. The primary winding consists of three layers (light grey, P_1 -

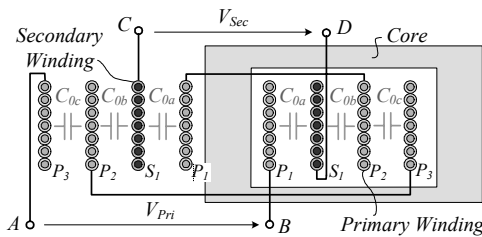


Figure 17. Transformer with interleaved primary and secondary winding

P_3) which are interleaved with one secondary layer (dark grey, S_1). First, an equivalent circuit consisting of 6 capacitors (Fig. 16) is calculated for each pair of layers as shown in Fig. 18 (where to each inner layer two capacitors are connected in parallel - e.g. C_{2a} and C_{1b} to the primary layer - according to the two basic cells on each side of the layer). The value of the static capacitance could be different for each layer.

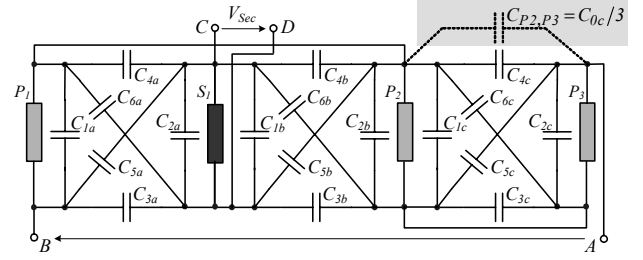


Figure 18. General equivalent circuit for transformer of Fig. 17

The layers P_2 and P_3 of the primary winding are not interleaved with the secondary winding and are connected directly. Thus, the interlayer capacitor $C_{P2,P3}$ simply could be modelled by one capacitor (instead of $C_{1c} - C_{6c}$) and calculated as described in sections III.A and III.B and shown in Fig. 18 in the grey shaded part.

In general the equivalent capacitor for two successive layers belonging to the same winding is directly calculated by $C_{Layer} = C_0/3$ or $C_{Layer} = C_0/3$ instead of using the six capacitor network (Fig. 16). Only two successive layers belonging to different windings must be modelled by the six capacitor network.

In the second step the equivalent layer capacitors are transformed to the connection of the winding (A and B in Fig. 17) by using the impedance transformation rule of transformers (24). This results in

$$C_{P2,P3} = \frac{C_{0c}}{3} \Rightarrow C_{Wdg} = C_{AB} = \left(\frac{2}{3}\right)^2 \cdot \frac{C_{0c}}{3}. \quad (31)$$

Furthermore, also all six capacitor networks are transformed to the connection of the winding.

This is done by writing the voltages of the six capacitors as function of the primary and secondary voltage V_1 and V_2 ,

$$\begin{aligned} V_{C1} &= (a-b) \cdot V_1 & V_{C2} &= (c-d) \cdot V_2 \\ V_{C3} &= -b \cdot V_1 + d \cdot V_2 + V_3 & V_{C4} &= -a \cdot V_1 + c \cdot V_2 + V_3 \\ V_{C5} &= -b \cdot V_1 + c \cdot V_2 + V_3 & V_{C6} &= -a \cdot V_1 + d \cdot V_2 + V_3 \end{aligned} \quad (32)$$

calculating the energy stored in the six original capacitors (Fig. 19) also as function of V_1 and V_2

$$W_{E,6C_org} = \frac{C_0}{12} \left[-V_{C1}^2 - V_{C2}^2 + 2V_{C3}^2 + 2V_{C4}^2 + V_{C5}^2 + V_{C6}^2 \right] \quad (33)$$

equating this energy to the energy which is stored in the six transformed capacitors (29). By comparing the coefficients of the different terms of V_1 , V_2 and V_3 the values of the six transformed capacitors could be calculated as function of the ratios a , b , c and d (34).

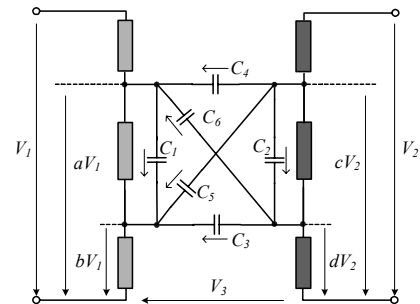


Figure 19. Transformation of six capacitor network

$$W_{E,6C_org} = W_{E,6C} \Rightarrow$$

$$\begin{aligned} C_1 &= C_0/6 \cdot (2a^2 + 2ab + 2b^2 - 3a - 3b) \\ C_2 &= C_0/6 \cdot (2c^2 - 3c - 3d + 2d^2 + 2cd) \\ C_3 &= C_0/6 \cdot (-3a + 2ac + ad - 3b + 2bd + bc - 3c - 3d + 6) \\ C_4 &= C_0/6 \cdot (2ac + ad + 2bd + bc) \\ C_5 &= C_0/6 \cdot (-2ac - ad - 2bd - bc + 3c + 3d) \\ C_6 &= C_0/6 \cdot (3a - 2ac - ad + 3b - 2bd - bc) \end{aligned} \quad (34)$$

All transformed six capacitor networks are finally connected in parallel. This is also true for the transformed equivalent layer capacitors of winding 1, which are in parallel to C_1 , and all transformed equivalent capacitors of winding 2, which are in parallel to C_2 . Thus, after combining all parallel capacitors to one capacitor a single six capacitor network modelling all parasitic capacitances results. For the considered example the result is shown in **Fig. 20** where it is assumed that all static layer capacitances ($C_{0a} = C_{0b} = C_{0c}$) are equal.

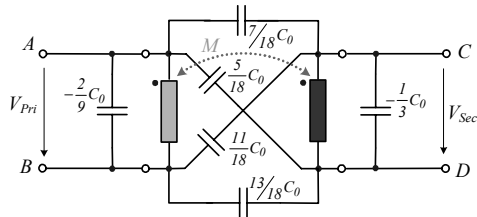


Figure 20. Resulting equivalent network for transformer of Fig. 17

V. EXPERIMENTAL VERIFICATION

In **Table II** the calculated results for the different approaches for one winding geometry and the two possible winding methods (standard and flyback) are given. Besides the analytic capacitance models also the results for the two empirical methods (6) / (13) are included. The largest value is obtained for orthocyclic turns since the distance between the wires is the smallest and the empirical values are close to this value. At the lower end of the range the values for the orthogonal turns and for parallel-plate and cylindrical model can be found since the distance between the wires is large.

C_{Layer}	Winding method	
	Standard	Flyback
Parallel-Plate (4)	140pF	105pF
Cylindrical (7)	140pF	105pF
Orthogonal (9)	133pF	99pF
Orthocyclic (11)	236pF	171pF
Orthocyclic II (14)	246pF	185pF
Empirical (plate) (6)	187pF	140pF
Empirical (cyclic) (11+13)	209pF	156pF

TABLE II- Comparison between layer capacitance models with $R_{L1} = 15mm$; $\delta = 30\mu m$; $r_0 = 0.75mm$; $z = 30$; $h = 0mm$; $\epsilon_D = 2.5$

In **Table III** the measurement and calculation results for four different high voltage transformers are given. The values, measured with an impedance analyser HP4294A from Agilent, agree well with the calculated average values of the transformers if the wire insulation is small in comparison to the wire diameter (HVT-1: $\delta / r_0 \approx 11\%$ and HVT-2: $\delta / r_0 \approx 10\%$). The range of values is a result of including the tolerances of the mechanical properties of the winding in the calculations.

For transformers, whose wire insulation is large in comparison to

the wire diameter (HVT-3: $\delta / r_0 \approx 50\%$ and HVT-2: $\delta / r_0 \approx 20\%$), the electric flux not only flows from the layer L_1 to the successive layer L_2 below but also to the layer L_3 , which is below layer L_2 . The flux is flowing through the relatively large areas of insulation between the wires of layer L_2 . Thus, for calculating the equivalent capacitance of a pair of layers one has to consider not only the next layer but also the subsequent. This must be considered in the equations and will be presented in a future paper.

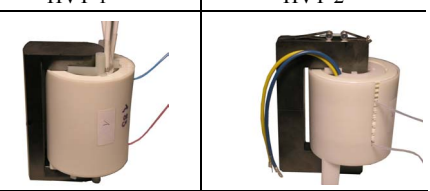
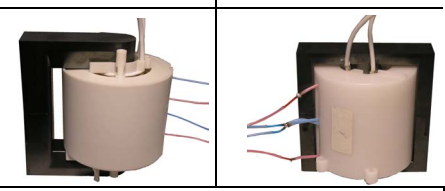
Type	HVT-1	HVT-2
		
Equivalent Secondary Winding Capacitor		
Measured	4.3pF	12.4pF
Orthogonal (9)	2.45... 2.78 ...3.14 pF	6.4... 7.3 ...8.3 pF
Orthocyclic (11)	4.12... 4.75 ...5.44 pF	10.7... 12.4 ...14.2 pF
Orthocyclic (11 +13)	3.91... 4.56 ...5.28 pF	9.66... 11.3 ...13.2 pF
Orthocyclic II (14)	4.55... 5.17 ...5.86 pF	11.9... 13.6 ...15.4 pF
Parallel-Plate (4)	3.68... 4.12 ...4.56 pF	9.7... 10.8 ...12.1 pF
Type	HVT-3	PT1
		
Equivalent Secondary Winding Capacitor		
Measured	7.15pF	4.2pF
Orthogonal (9)	0.99... 1.16 ...1.35 pF	0.83... 1.31 ...3.35 pF
Orthocyclic (11)	1.40... 1.70 ...2.03 pF	1.25... 2.15 ...6.05 pF
Orthocyclic (11 +13)	1.05... 1.31 ...1.57 pF	1.26... 2.16 ...6.1 pF
Orthocyclic II (14)	1.81... 2.09 ...2.41 pF	1.60... 2.44 ...6.35 pF
Parallel-Plate (4)	1.29... 1.51 ...1.75 pF	1.25... 2.01 ...4.17 pF

TABLE III – Experimental results for four high-voltage transformers

VI. CONCLUSION

A complete survey of the different calculation methods for parasitic transformer capacitances is given and general equations are added. Based on the compiled equations a simple modelling procedure for the parasitic capacitances of inductors and transformers is presented. The different calculations methods are compared and verified by FEA simulations and measurement results for high-voltage transformers.

As proofed by the measurement results the equivalent capacitor could be calculated by the presented procedures and predicted without building the transformer. The parasitic capacitance, which is in parallel to the windings of the transformer, could be used as parallel capacitor in a series-parallel resonant DC-DC-converter as proven by experiment.

Due to the admissible page count of this paper the influence of the core and shields on the equivalent winding capacitor has been neglected. The corresponding equations and measurement results will be presented in a future paper.

REFERENCES

- [1] G. A. Ward and A. J. Forsyth, „Topology selection and design trade-offs for multi-kW telecom DC power supplies“, Power Electronics, Machines and Drives, International Conference on Conf. Publ. No. 487), 4-7 June 2002 pp. 439-444.
- [2] F. Cavalante, J. W. Kolar, „Design of a 5kW high output voltage series-parallel resonant DC-DC converter“, Power Electronics Specialist, PESC '03 IEEE 34th Annual Conference on, Volume: 4, June 15-19, pp. 1807-1814.
- [3] S. Dieckerhoff, M. J. Ruan, R. W. De Doncker, „Design of an IGBT-based LCL-resonant inverter for high-frequency induction heating“, Industry Applications Conference, Thirty-Fourth IAS Annual Meeting, Conference Record of the 1999 IEEE, Volume 3, 3-7 Oct. 1999, pp. 2039 – 2045.
- [4] A. K. S. Bhat, S. B. Dewan, „Analysis and design of a high-frequency resonant converter using LCC-type commutation“, IEEE Transaction on Power Electronics, vol.2, No.4, 1987, pp. 291-300.
- [5] R. L. Steigerwald, „A comparison of half-bridge resonant converter topologies“, Power Electronics, IEEE Transactions on, Volume: 3 Issue: 2, April 1988 pp. 174-182.
- [6] J. Biela, J.W. Kolar, „Analytic Design Method for (Integrated-) Transformers of Resonant Converters using Extended Fundamental Frequency Analysis“ Proceedings of the 5th International Power Electronics Conference (IPEC), Niigata, Japan, April 4 - 8, 2005.
- [7] J. Biela, J.W. Kolar, „Design of high power Electromagnetic Integrated Transformers by means of Reluctance Models and a structured Survey of Leakage Paths“ Proceedings of the 35th IEEE Power Electronics Specialists Conference, Aachen, Germany, June 20 - 25, CD-ROM, ISBN: 07803-8400-8 (2004).
- [8] M. C. Smit, J. A. Ferreira and J. D. van Wyk, „Application of transmission line principles to high frequency power converters“, Power Electronics Specialists Conference, PESC '92 Record, 23rd Annual IEEE, 29 June-3 July 1992, pp. 1423-1430 vol.2.
- [9] J. T. Strydom, „Electromagnetic Design of Integrated Resonator-Transformers“, Ph.D. Thesis, Rand Afrikaans University, South Africa, 2001.
- [10] W. T. Duerdoh, „Equivalent Capacitances of Transformer Windings“, Wireless Engineer, vol. 23, June 1946, Pp. 161 – 167.
- [11] J. Koch, „Berechnung der Kapazität von Spulen, insbesondere in Schalenkernen“, Valvo Berichte, Band XIV, Heft 3, 1968, pp. 99 – 119.
- [12] A. Massarini, M.K. Kazimierzczuk, „Self-capacitance of inductors“, Power Electronics, IEEE Transactions on, Vol. 12, Issue: 4, July 1997, pp. 671 – 676.
- [13] W. Schröder, „Berechnung der Eigenschwingungen der doppellagigen langen Spule“, Archiv für Elektrotechnik, Band XI, Heft 6, 1922, pp. 203 – 229.
- [14] B. Cogitore, J.-P. Keradec, J. Barbaroux, „The two-winding transformer: an experimental method to obtain a wide frequency range equivalent circuit“, Trans action on Instrumentation and Measurement, Vol. 43, Issue: 2, April, 1994, pp. 364 – 371.
- [15] E. Laveuve, J. P. Keradec, M. Bensoam, „Electrostatic of sound components: analytical results, simulation and experimental validation of the parasitic capacitance“, Conference Record of the Industry Applications Society Annual Meeting, Vol. 2, Sept. 28 - Oct. 4, 1991, pp. 1469 – 1475.
- [16] P. Wallmeier, „Automatisierte Optimierung von induktiven Bauelementen für Stromrichter-anwendungen“, Shaker-Verlag, Aachen, 2001, pp. 102-107.
- [17] L. Oestergaard, „Modelling and Simulation of the Diode Split Transformer“, Dissertation, Faculty of Engineering and Science at Aalborg University, 1999, pp. 139 – 169.
- [18] H. Zuhrt, „Einfache Näherungsformel für die Eigenkapazität mehrlagiger Spulen“, Elektrotechnische Zeitschrift, Heft 27, 1934, pp. 662 – 665.
- [19] J. A. Collins, „An Accurate Method for Modelling Transformer Winding Capacitances“, Industrial Electronics Conference, 1990, pp. 1094 – 1099.
- [20] E. C. Snelling, „Soft Ferrites: Properties and Applications“, Butterworths, London, 1988, pp. 330 – 335.
- [21] M. Albach, J. Lauter, „The Winding Capacitance of Solid and Litz Wires“, European Power Electronics Conference, EPE'97, Trondheim, pp. 2.001 – 2.005.
- [22] R. Feldtkeller, „Theorie der Spulen und Übertrager“, S. Hirzel Verlag, Stuttgart, 3. Auflage, 1958
- [23] T. Duerbaum, G. Sauerlaender, „Energy based Capacitance Model for Magnetic Devices“, Applied Power Electronics Conference and Exposition, APEC 2001, Volume: 1, March 4-8, pp. 109 – 115.
- [24] R. Prieto, R. Asensi, J.A. Cobos, O. Garcia, J. Uceda, „Model of the capacitive effects in magnetic components“, 26th Power Electronics Specialists Conference PESC '95, Vol. 2, June 18-22, 1995, pp. 678 – 683.
- [25] N. R. Grossner, I. S. Grossner, „Transformers for Electronic Circuits“, 2nd Edition, Mc Graw-Hill Book Company, New York, 1983.
- [26] W. M. Flanagan, „Handbook of Transformer Design & Applications“, 2nd Edition, McGraw-Hill, New York, 1993, pp. 10.6 – 10.9.
- [27] K.A. Macfadyen, „Small Transformers and Inductors“, Chapman & Hall LTD, London, 1953, pp. 55-60.
- [28] Members of the staff of the Department of Electrical Engineering MIT, „Magnetic Circuits and Transformers“, J. Wiley & Sons, New York / Chapman & Hall, London, 1944.
- [29] F. Ollendorf, „Potentialfelder der Elektrotechnik“, Verlag von Julius Springer, Berlin, 1932, pp. 337-340.
- [30] T. Duerbaum, „Capacitance Model for Magnetic Devices“, 31st Power Electronics Specialist Conference PESC, Vol. 3, June 18-23, 2000, pp. 1651 – 1656.
- [31] T. Duerbaum, „Layer based Capacitance Model for Magnetic Devices“, Proceedings of the 8th European Conference on Power Electronics EPE'99, 1999.
- [32] F. Blache, J.-P. Keradec, B. Cogitore, „Stray capacitances of two winding transformers: equivalent circuit, measurements, calculation and lowering“, Conference Record of the Industry Applications Society Annual Meeting, Vol. 2, October 2-6, 1994, pp. 1211 – 1217.
- [33] A. Schellmanns, J.-P. Keradec, J.-L. Schanen, K. Berrouche, „Representing electrical behaviour of transformers by lumped element circuits: a global physical approach“, Conference Record of the 34th Industry Applications Conference, Vol. 3, October 3-7, 1999, pp.2100 – 2107.
- [34] A. Massarini, M.K. Kazimierzczuk, „Modelling the Parasitic Capacitance of Inductors“, 16 Capacitor and Resistor Technology Symposium CARTS 96, 1996, March 11-15, pp. 78 – 85.
- [35] A. Massarini, M.K. Kazimierzczuk, G.Gandi, „Lumped Parameter Models for Single- and Multiple-Layers Inductors“, 27th Power Electronics Specialists Conference PESC '96, Vol. 1, June 23-27, 1996, pp. 295 – 301.
- [36] M. Gehnen, „Messung und Modellierung des Schwingungsverhaltens von Leistungstransformatoren zur Beurteilung kritischer Resonanzfälle“, Shaker-Verlag, Aachen, 1994, pp. 9-15.
- [37] M.A. Perez, C. Blanco, M. Rico, F.F. Linera, „A new topology for high voltage, high frequency transformers“, 10th Applied Power Electronics Conference and Exposition APEC '95, Vol. 2, Issue: 0, March 5-9, 1995, pp. 554 – 559.
- [38] W. T. McLyman, „Transformer and Inductor Design Handbook“, Marcel Dekker, New York and Basel, 2004.
- [39] L. F. Casey, A.F. Goldberg, M.F. Schlecht, „Issues regarding the capacitance of 1-10 MHz transformers“, 3rd Applied Power Electronics Conference and Exposition APEC '88, Feb. 1-5, 1988, pp. 352 – 359.
- [40] M. Xinkui; Chen Wie, „More precise model for parasitic capacitances in high-frequency transformer“, 33rd Power Electronics Specialists Conference PESC'02, Vol. 2, June 23-27, June 2002, pp. 1054 – 1057.
- [41] J. Schutz, J. Roudet, A. Schellmanns, „Transformer modelling in EMC applications“, 33rd Industry Applications Conference, Vol. 2, October 12-15, 1998, pp. 1005 – 1010.
- [42] J. Leohold, „Untersuchung des Resonanzverhaltens von Transformatorwicklungen“, Dissertation at the University of Hanover, 1984.
- [43] E. Buckow, „Berechnung des Verhaltens von Leistungstransformatoren bei Resonanzanregung und Möglichkeiten des Abbaus innerer Spannungsüberhöhungen“, Dissertation at the Technical University of Darmstadt, 1986.
- [44] J. C. Hubbard, „On the Effect of Distributed Capacity in Single Layer Solenoids“, Physical Review, Vol. 9, June, 1917, pp. 529-541.
- [45] Hai Yan Lu, Jian Guo Zhu, S.Y.R. Hui, „Experimental determination of stray capacitances in high frequency transformers“, IEEE Transaction on Power Electronics, Vol. 18, Issue: 5, Sept., 2003, pp. 1105 – 1112.
- [46] J.M. Prieto, A. Fernandez, J.M. Diaz, J.M. Lopera, J. Sebastian, „Influence of transformer parasitics in low-power applications“, 14th Applied Power Electronics Conference and Exposition APEC '99, Vol. 2, March 14-18, 1999, pp. 1175 – 1180.
- [47] K. KrefB, „Untersuchungen zum elektrischen Resonanzverhalten einlagiger Luftspulen bei hohen Frequenzen“, Dissertation at the technical University of Darmstadt, 1991.
- [48] A. J. Palermo, „Distributed Capacity of Single-Layer Coils“, Proceedings of the Institute of Radio Engineers, Vol. 22, No. 7, July, 1934 pp. 897 – 905.
- [49] G.Gandi, M.K. Kazimierzczuk, A. Massarini, U. Reggiani, „Stray Capacitances of Single-Layer Solenoid Air-Core Inductors“, IEEE Transaction on Industry Applications, Vol.35, No.5, 1999, pp. 1162-1168.
- [50] G. Grandi, M.K. Kazimierzczuk, A. Massarini, U. Reggiani, „Stray capacitances of single-layer air-core inductors for high-frequency applications“, Conference Record of the Industry Applications Conference IAS '96, Vol. 3, October 6-10, 1996, pp.1384 – 1388.
- [51] R. G. Medhurst, „H.F. Resistance and Self-Capacitance of Single-Layer Solenoids“, Wireless Engineer, vol. 24, March 1947, pp. 80 – 92.
- [52] R. Körger, R. Unbehauen, „Elektrodynamik“, B. G. Teubner, Stuttgart.

Appendix A - List of Symbols

ϵ_D	Dielectric constant of wire insulation	k	Number of turns in one incomplete layer
ϵ_F	Dielectric constant of foil between layers	L_L	Length of coil (or sum of sections)
$\epsilon_{r,m}$	Effective dielectric constant	$l_{w,m}$	Mean turn length of two the considered layers
δ	Thickness of wire insulation	N_S	Number of strands of litz wire
δ_{twist}	Thickness of outer insulation of litz wire	N_{Layer}	Number of all layers of one winding
δ_{Wire}	Thickness of insulation of a single strand	$N_{L,i}$	Number of turns in layer i
b_{Sec}	Breadth of winding section	N_{Sec}	Number of Sections
C_0	Static capacitance between two layers	R_{L1}	Radius of inner layer of considered pair of layers
C_{Layer}	Equivalent capacitor between two layers	R_{L2}	Radius of outer layer of considered pair of layers
C_{Sec}	Equivalent capacitor of one section	d_i / r_i	Diameter / Radius of wire without insulation
C_{Wdg}	Equivalent capacitor of the whole winding	d_0 / r_0	Diameter / Radius of wire including insulation
$C_{1,6}$	Equivalent capacitor general model	V_{LL}	Voltage between two successive layers of one winding
d	Distance between successive turns	V_{Wdg}	Voltage of one winding
$d_{w,0}$	Diameter of a single strand with insulation	V_{tt}	Voltage between two successive turns
d_{Sec}	Distance between two successive sections	$W_{E,LL}$	Electrical energy stored between two layers
d_u	Distance between two successive turns	$W_{E,6C}$	Electrical energy stored in equivalent six capacitor network
h	Thickness of foil or distance between layers	$W_{E,Wdg}$	Electrical energy stored in one winding
d_{eff}	Effective distance between two layers	z	Number of turns in one complete layer